Scientific Report

SOURCE DATA | TRANSPARENT PROCESS

EMBO reports

# Potent degradation of neuronal miRNAs induced by highly complementary targets

Manuel de la Mata[1], Dimos Gaidatzis[1,2], Mirela Vitanescu[1,†], Michael B Stadler[1,2,3], Corinna Wentzel[4,‡], Peter Scheiffele[4], Witold Filipowicz[1,3,*] & Helge Großhans[1,**]

## Abstract

**MicroRNAs (miRNAs) regulate target mRNAs by silencing them. Reciprocally, however, target mRNAs can also modulate miRNA stability. Here, we uncover a remarkable efficacy of target RNA-directed miRNA degradation (TDMD) in rodent primary neurons. Coincident with degradation, and while still bound to Argonaute, targeted miRNAs are 3′ terminally tailed and trimmed. Absolute quantification of both miRNAs and their decay-inducing targets suggests that neuronal TDMD is multiple turnover and does not involve co-degradation of the target but rather competes with miRNA-mediated decay of the target. Moreover, mRNA silencing, but not TDMD, relies on cooperativity among multiple target sites to reach high efficacy. This knowledge can be harnessed for effective depletion of abundant miRNAs. Our findings bring insight into a potent miRNA degradation pathway in primary neurons, whose TDMD activity greatly surpasses that of non-neuronal cells and established cell lines. Thus, TDMD may be particularly relevant for miRNA regulation in the nervous system.**

**Keywords** cooperativity; miRNA target; miRNA turnover; non-templated RNA 3′-end nucleotide additions; primary hippocampal neurons
**Subject Category** RNA Biology
**DOI** 10.15252/embr.201540078 | Received 8 January 2015 | Revised 21 January 2015 | Accepted 26 January 2015 | Published online 27 February 2015
**EMBO Reports (2015) 16: 500–511**

## Introduction

MicroRNAs constitute a large family of ~21-nucleotide-long RNAs that silence mRNAs in animals and plants. They function by binding to imperfectly complementary sequences present largely in the 3′-untranslated regions (UTRs) of target mRNAs, causing mRNA translational repression, deadenylation, and degradation [1]. As posttranscriptional regulators, they are well suited for induction of rapid and spatially localized changes in gene expression. Consistently, miRNA maturation can be controlled at various steps to provide tight control over the levels of individual or groups of miRNAs [1]. However, dynamic changes in target gene activity in response to alterations in miRNA biogenesis rates require mechanisms of active and regulated miRNA turnover [2]. Indeed, although miRNAs are generally highly stable in various cell types, with half-lives extending to days [3–6], they are substantially less stable in neurons [7–9]. Moreover, viral infection and cell cycle status were found to destabilize certain miRNAs [10–14].

miRNAs function in association with Argonaute (AGO) proteins, the core components of the RNA-induced silencing complex (RISC). Argonautes contain specific protein pockets that bind, and thus essentially shield, the 5′- and 3′-termini of miRNAs. Consequently, selective recognition, release, and degradation of a specific miRNA represent a mechanistic challenge. The recent discovery that binding of highly complementary RNAs may destabilize miRNAs [15] may provide a solution to this issue. This and other studies [3,12] demonstrated that target mRNAs or non-coding RNAs trigger 3′-end "tailing," that is, addition of non-templated nucleotides; 3′-to-5′ trimming; and decay of highly complementary miRNAs. In the following, we will refer to this process as target RNA-directed miRNA degradation or TDMD.

The mechanisms underlying, and the constraints acting on, TDMD remain largely unknown. For instance, it is unknown whether tailed and trimmed miRNA species are true intermediates of miRNA degradation or the outcomes of independent, parallel processes, and whether these processes occur on RISC or subsequent to unloading of miRNAs from Ago. Moreover, the fate of the TDMD-inducing RNA has not been investigated and may or may not involve co-degradation with the targeted miRNA. Co-degradation would limit target availability and the ability of TDMD to clear abundant miRNAs.

Certain viruses employ TDMD to degrade host miRNAs, some of which have antiviral activities [10,12,13,16], but physiological functions of TDMD remain to be identified. Because dynamic miRNA regulation seems crucial for the nervous system [17], we explored the

1 Friedrich Miescher Institute for Biomedical Research, Basel, Switzerland
2 Swiss Institute of Bioinformatics, Basel, Switzerland
3 University of Basel, Basel, Switzerland
4 Biozentrum, University of Basel, Basel, Switzerland
*Corresponding author. Tel: +41 61 697 6993; E-mail: witold.filipowicz@fmi.ch
**Corresponding author. Tel: +41 61 697 6675; E-mail: helge.grosshans@fmi.ch
†Present address: Department of Anaesthesiology and Pain Medicine, Inselspital, University of Bern, Bern, Switzerland
‡Present address: Institute of Molecular Life Sciences, University of Zurich, Zurich, Switzerland

occurrence of TDMD in rodent neurons. We find that TDMD is not only operational but also particularly effective in primary neurons. We provide detailed characterization of the TDMD process and discuss its potential importance for regulation of miRNAs in neurons.

## Results

### Target mRNAs induce efficient decay of cognate miRNAs in neurons

Because neurons appear to make extensive use of miRNAs and their dynamic regulation, we reasoned that they might constitute a good model to investigate TDMD. To test this possibility, we constructed lentiviruses expressing target mRNAs with binding sites for miR-124 and miR-132, respectively, two miRNAs that are endogenously expressed in neurons [7]. Target mRNAs encode GFP and contain a 3′-untranslated region (UTR) with four binding sites (4× target) that pair extensively with the seed and 3′-end of the miRNAs but contain a central bulge. As a control, we generated an identical set of targets (referred to as mut targets), in which we mutated the seed-binding region (Fig 1A). Use of the neuron-specific human synapsin (Syn) promoter excludes transgene expression from glial cells, which are present in small amounts in primary hippocampal cell cultures.

We transduced lentiviruses at a multiplicity of infection (MOI) of 1–5 into dissociated rat hippocampal neurons at day 9 of *in vitro* culture (DIV9) and extracted total RNA at 6 days post-infection (DIV15). When measuring miRNA levels by reverse transcription–quantitative polymerase chain reaction (RT–qPCR), we found that neurons expressing the 4× target displayed significant, up to eightfold reduction in the cognate miRNA levels relative to cells expressing a mut target or no target (Fig 1B). As thoroughly addressed below, miR-132 levels decreased more than miR-124 levels. We confirmed the downregulation of miR-132 by Northern blotting (Fig 1C) and sequencing (Fig 1D; see below), ruling out that the miRNAs remain present but are inaccessible to amplification by RT–qPCR.

To test the specificity and robustness of the effect, we sequenced small RNAs isolated from infected neurons. This revealed that the miR-132 target affected exclusively miR-132 (Fig 1D). Moreover, we found that the effect is context-independent since another miR-132 target bearing unrelated coding and 3′-UTR sequences also drove miRNA degradation (Supplementary Fig S1A and B; Materials and Methods). Finally, to eliminate the possibility that reduced accumulation of mature miRNA was a consequence of changes in transcription and/or maturation of targeted miRNAs, we measured levels of corresponding pri-miRNAs and miRNAs* (passenger strands). The levels of both remained unchanged by the target mRNAs, thus confirming that the reduction in the guide strand occurs after Dicer-mediated processing (Fig 1D–F).

Taking all these data together, we conclude that target mRNAs effectively and specifically decrease the levels of their cognate miRNAs in hippocampal neurons through a TDMD-like process.

### Target-induced decay is highly correlated with tailing and trimming of targeted miRNAs in neurons

To determine whether miRNA 3′-to-5′ trimming and 3′-end tailing occurred in neurons as it does in other instances of TDMD [3,12,15], we used small RNA sequencing to identify miR-132 isoforms in neurons transduced with the targets described below. We focused on miR-132 for two reasons. First, it exhibits more effective TDMD relative to miR-124 (Fig 1B and see below). Second, tailing was previously reported to involve mostly the addition of adenosines (A) and uridines (U). Because the first two nucleotides 3′ of the mature miR-124 are AA in all three *Mir124* loci, a distinction between templated and non-templated 3′ A-additions would not be feasible.

We performed isoform-specific quantification for miR-132 by counting the number of occurrences of each unique sequence matching the first 18 nt of miR-132. This confirmed that the most abundant species, corresponding to the annotated mature isoform [18], decreased tenfold after transduction of the 4× target (Supplementary Fig S1C), consistent with measurements obtained by RT–qPCR and Northern blot (Supplementary Fig S1D and E). Interestingly, we also detected species with 3′ non-templated tails, some of which accumulate in the presence of a 4× target for miR-132 but not in the presence of either a mut target, seed-only pairing target, or a target specific for miR-124 (Supplementary Fig S1C). Most of the detected tailed species contain adenosines and/or uridines, with fewer cytidines and guanosines being added. Trimmed species were also detected, although most of them were reduced and did not accumulate upon expression of a 4× target.

To achieve a better understanding of the dynamics of tailing, trimming, and miRNA decay, we performed a time-course analysis. To this end, we used an inducible promoter to drive expression of a 4× target of miR-132. Sequencing of RNA samples extracted after different times of target induction followed by isoform-specific quantification revealed a rapid initiation of TDMD in that mature miR-132 levels already declined by 8–24 h of induction (Fig 2A), reflecting similar target RNA induction dynamics (Supplementary Fig S2E). Whereas the levels of the mature miRNA declined progressively, other less abundant isoforms displayed apparently distinct expression trends (Fig 2A and C). Thus, tailed species started to accumulate gradually as early as 8 h after target induction, correlating with the decrease in mature miRNA levels (Fig 2A). Depending on tail length and composition, maximum accumulation was detected starting at 24 h with levels staying strongly elevated at 72 h. By contrast, trimmed species as well as a subset of species with mostly short tails tended to exhibit expression patterns that were comparable to that seen for mature miR-132, that is, mostly stable expression during the first 8 h, followed by a detectable decline in levels at 24 and 72 h. We quantified the association between the change in isoform expression and tailing by calculating the Spearman rank correlation between the isoform rank in Fig 2A and the corresponding isoform length. The correlation was 0.85 ($P$ = 1.3e-51). From this result, we conclude that expression of tailed species shows a strong temporal correlation with the decay of the mature miRNA, consistent with the idea that they could be true intermediates of the miRNA decay pathway.

### Target mRNAs induce miRNA tailing on Ago2

The fact that highly complementary RNA targets induce 3′-tailing and degradation of miRNAs could be explained by a sequence of events where targets first induce unloading of miRNA from Argonaute proteins [19] followed by tailing and degradation of released

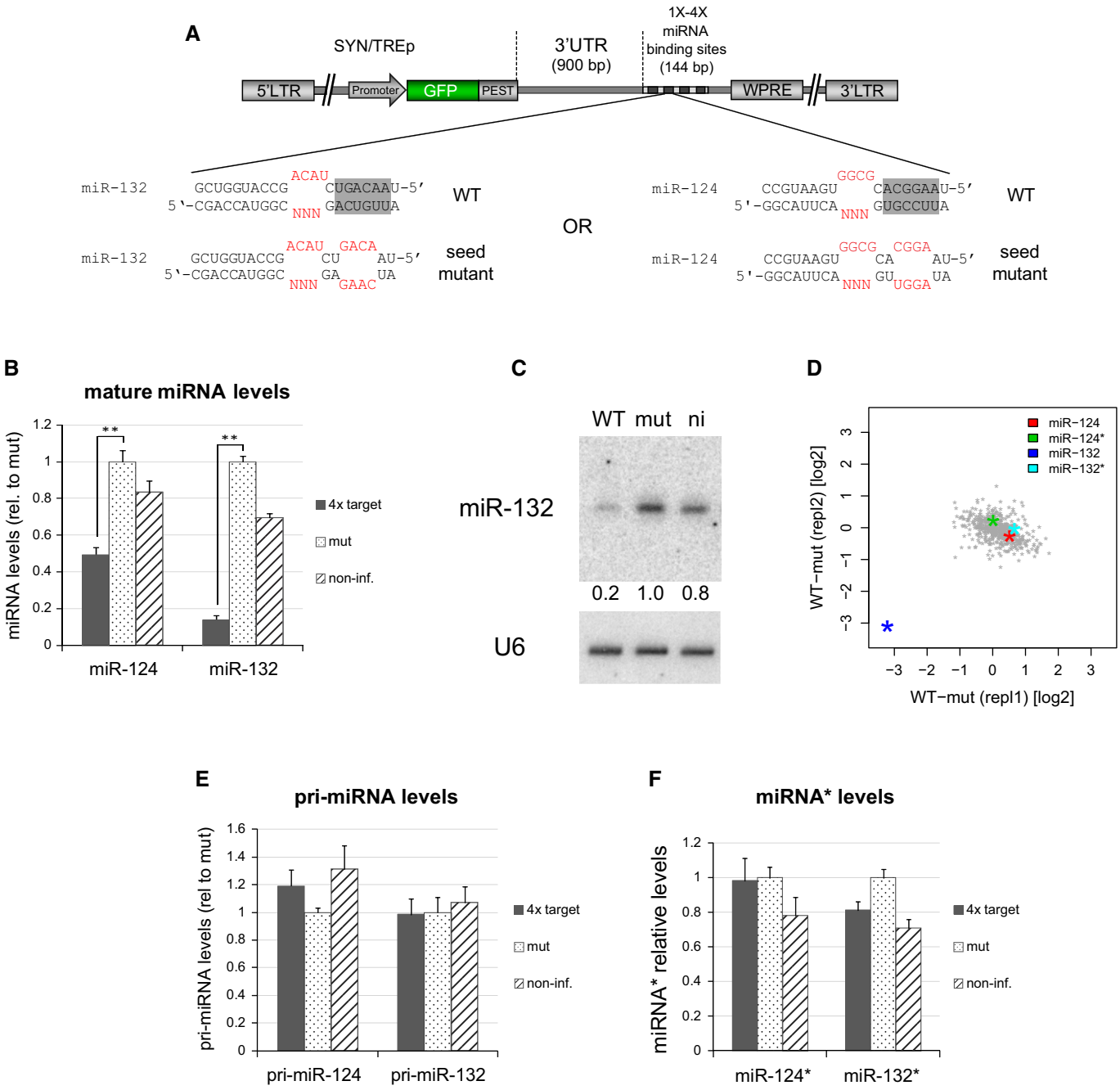


**Figure 1. Target mRNAs transcribed from the synapsin promoter induce efficient decay of cognate miRNAs in rat primary hippocampal neurons.**

A Schematic illustration of the vectors used in this work. Lentiviral transgenes express GFP-PEST, followed by a fragment of the CaMKIIα 3′-UTR, and 1 or 4 miRNA binding sites against candidate miRNAs. SYN, human synapsin promoter; TREp, tetracycline-inducible promoter; WPRE, woodchuck hepatitis virus posttranscriptional control element; LTR, long terminal repeats. Seed-pairing region is highlighted in gray. Unpaired nucleotides are depicted in red. "*N*" indicates variable nucleotide sequence among individual target sites.

B RT–qPCR was used to determine the levels of the indicated miRNAs in neurons in the presence of the indicated targets; shown are means ± s.e.m.; $n = 11$ (for miR-124) and $n = 12$ (for miR-132). $^{**}P < 0.01$ ($P = 5e\text{-}7$ for miR-124; $P = 1e\text{-}16$ for miR-132; calculated by an independent two-sample *t*-test.).

C miR-132 levels determined by Northern blot analysis in non-infected neurons (ni) or neurons infected with targets bearing 4× WT or seed-mutant binding sites. Relative miRNA levels are indicated below the lanes.

D Scatter plot from small RNA sequencing data comparing $\log_2$ expression values in neurons infected with WT versus mut targets of miR-132. The transgenes affect only the targeted miRNA without any non-specific effect on non-related miRNAs.

E, F RT–qPCR was used to determine the levels of the indicated (E) pri-miRNAs and (F) passenger strand miRNAs (miRNA*) in neurons in the presence of the indicated targets. "non-inf." are non-infected control cells. U6 RNA levels were used to normalize miRNA levels. Shown are means ± s.e.m.; $n = 4$ in (E), $n = 4$ in (F).

Source data are available online for this figure.

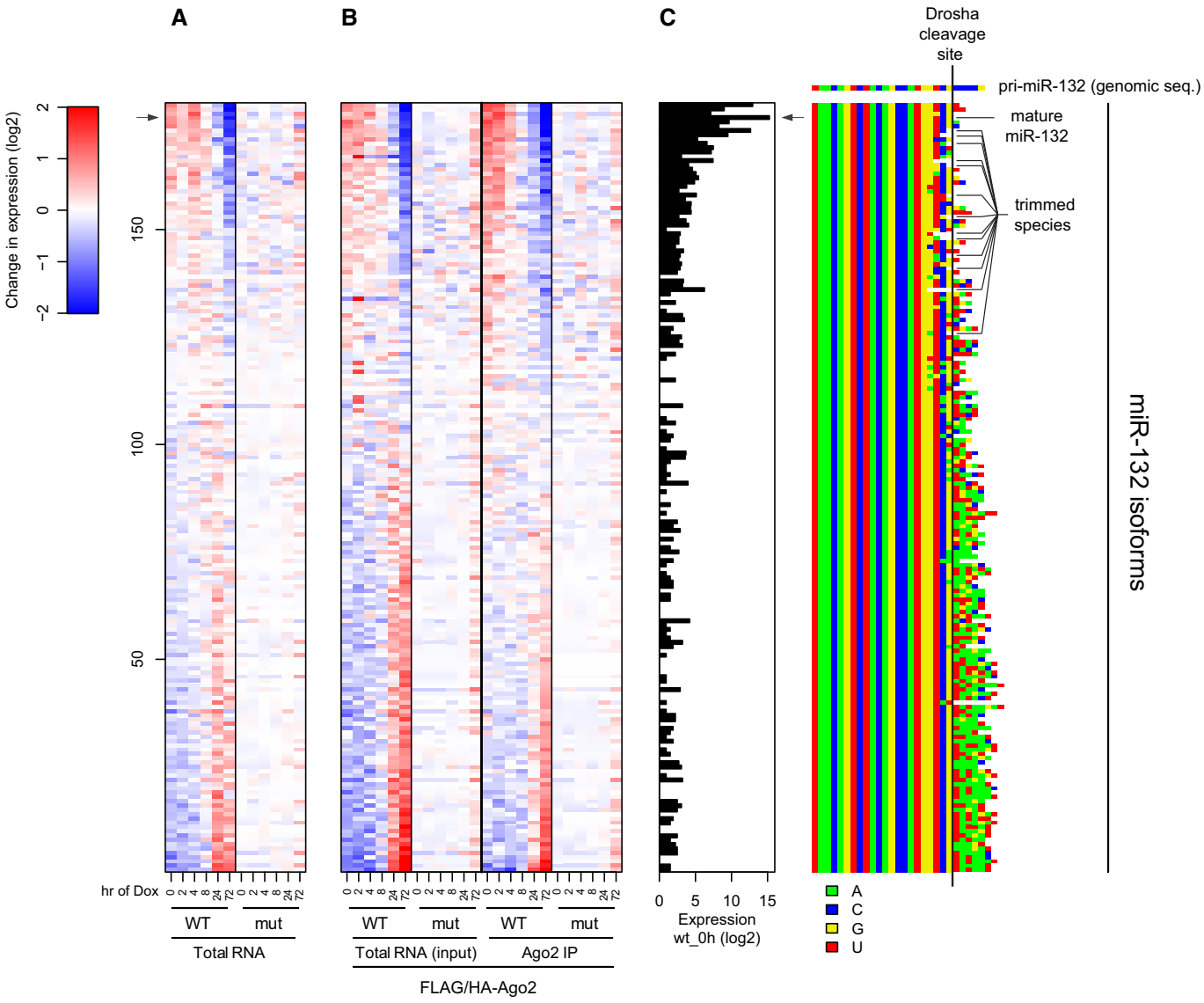


**Figure 2. Target mRNAs induce tailing and trimming on Ago2-loaded miRNAs.**

A, B Sequencing analysis of miR-132 species in (A) total RNA from hippocampal neurons (DIV16) transduced with an inducible target against miR-132 (4× WT or mut target), or (B) total RNA (input) or Ago2-immunoprecipitated RNA (Ago2 IP) from hippocampal neurons (DIV16) co-transduced with lentiviruses expressing FLAG/HA-Ago2 and an inducible target against miR-132 (4× WT or mut target). Targets were induced for the indicated times with Dox. The heatmaps depict isoform-specific $\log_2$ relative expression levels, mean-normalized across each of the individual six time courses. The isoforms are sorted based on the first principal component calculated from the full dataset. The slight upregulation of some species in the mutant controls at 72 h of induction may reflect indirect effects of long-term transgene expression. Thirty-four isoforms, which showed > fourfold higher levels for the WT than for the mut target at 0 h due to leaky expression of the inducible target (Supplementary Fig S2E), were filtered out. Their expression does not change significantly at later time points, suggesting saturated induction and thus no informative value for the dynamics of the system.

C Left panel: Bar plot indicating the absolute $\log_2$ expression levels measured in total RNA at 0 h time point in the presence of the 4× WT target, averaged over the two experiments. Right panel: Isoform sequences displayed by color-coding. A solid black line indicates the Drosha cleavage site that generates the 3′-end of miR-132-3p and thus the limit of genomically encoded sequence.

Data information: Arrows in (A) and (C) indicate the values corresponding to mature miR-132.

miRNAs. Alternatively, 3′-tailing could be induced while miRNAs are still loaded on Ago and this in turn could lead to unloading and/or degradation of miRNAs. To distinguish between these possibilities, we co-transduced neurons with lentiviral transgenes expressing FLAG/HA-Ago2 together with an inducible 4× target against miR-132. A time-course analysis was then performed by inducing transcription for different times, followed by anti-FLAG immunoprecipitation (IP) of Ago2 with associated RNA. By Western blot analysis, we detected Ago2 but not Actin in the IP fraction, while RT–qPCR analysis confirmed that miRNAs but not U6 RNA were present in the Ago2 IP material (Supplementary Fig S2A–C). To analyze the miR-132 isoform profiles in the input and Ago2 IP

fractions, we performed small RNA sequencing in both fractions (Fig 2B). Notably, expression of the tagged Ago2 together with the 4× target did not appreciably alter the miR-132 isoform patterns in input samples relative to neurons infected with the 4× target alone (Fig 2A and B), despite an eightfold increased abundance of FLAG/HA-Ago2 over endogenous Ago2 mRNA. Moreover, we observed a striking similarity in the miR-132 isoform pattern between total RNA (input) and Ago2-associated RNA. In both fractions, a variety of 3′-tailed species accumulate in a highly dynamic fashion and with different kinetics in response to target induction. Most tailed species contain non-templated A/U nucleotides with some trimmed and apparently re-tailed species also present. When considered together with the transient enrichment of the target RNA on Ago2 (Supplementary Fig S2E–G), these results indicate that target mRNAs trigger tailing of miRNAs while miRNAs are bound by Ago proteins. Hence, it appears that the miRNA degradation machinery can act in close proximity to, or in association with, RISC, perhaps explaining the rapid and efficient miRNA turnover that we observe.

### Canonical miRNA target sites cannot induce nor compete with TDMD

Natural miRNA binding sites in animals generally base pair with limited 3′-proximal complementarity to their cognate miRNAs [20]. *In vitro*, TDMD requires extensive but not full complementarity, and conventional miRNA binding sites do not alter miRNA stability [15]. To define the base-pairing requirements that mediate TDMD in neurons, we generated target mRNAs carrying miRNA binding sites with various pairing architectures (Figs 1A and 3A). Since a single target site suffices for efficient degradation of miR-132 (see below), we utilized targets with only a single site (1× targets). This analysis revealed that sites with central bulges of up to five nucleotides triggered efficient TDMD of miR-132, whereas a further increase in the bulge size to seven nucleotides abolished the effect (Fig 3B). TDMD activity relied also extensively on base-pairing to the 3′-end of the miRNA: A two-nucleotide mismatch to the 3′-end of the miRNA reduced the extent of TDMD from tenfold to threefold, and a total of four mismatches completely abolished TDMD, when assayed in the context of a target with a 4-nt bulge (Fig 3B).

Collectively, these results imply that typical miRNA binding sites, which lack extended complementarity to the miRNA 3′-end, would not be efficient triggers of TDMD. Consistent with this notion, none of three different 3′-UTRs from genes reported to be natural targets of miR-132-induced TDMD [21–23] (Supplementary Fig S3A and B). Similarly, five bioinformatically predicted miR-132 binding sites with canonical architecture [24] were unable to trigger TDMD when inserted together into the target reporter 3′-UTR expressed in hippocampal neurons (Supplementary Fig S3C and D).

Although the canonical targets thus appear to be unable to induce TDMD, it seemed feasible that they might compete with the extensively complementary target for miRNA binding. To test this possibility, we co-expressed TDMD-inducing 1× or 4× targets (Fig 3C and E) bearing highly complementary binding sites with targets containing mimics of endogenous canonical sites (canonical targets). Unexpectedly, TDMD efficiency was either not affected by co-expression of a canonical target (Fig 3C and D) or the effect of the canonical target was comparable to that of the mutant control (Fig 3E and F).

We conclude from these results that extensive 3′-end pairing to the miRNA is required to induce efficient TDMD and that canonical miRNA binding sites can neither induce miRNA decay themselves nor compromise TDMD induced by highly complementary targets.

### miRNA abundance affects a balance between TDMD and miRNA-mediated target degradation

Since the above results suggested that competition between endogenous and highly complementary targets could not account for the differences in TDMD activity toward miR-124 versus miR-132, we explored whether miRNA abundance was instead a critical factor. In order to avoid technical biases inherent to relative quantification methods, we utilized synthetic miRNA standards to achieve absolute quantification; that is, determine the number of miR-124 and miR-132 molecules in a given amount of total RNA. This revealed that miR-124 was approximately one order of magnitude more abundant than miR-132 (Fig 4A; Materials and Methods). Consistent with this finding, miR-124 but not miR-132 silenced a target reporter very effectively (Supplementary Fig S4A and B).

To test whether the differences in miRNA levels could indeed explain the differences in the TDMD effect, we generated highly complementary 4× targets against four additional neuron-specific miRNAs, which we had selected to cover a broad range of expression levels based on absolute quantification. To relate these levels to concentrations of TDMD-inducing target mRNAs, we also quantified the number of mut target mRNA molecules (as a measure of baseline levels of both WT and mut targets) per hippocampal neuron (Materials and Methods). Three of the six selected miRNAs are expressed at lower molar concentrations relative to this mRNA level, whereas three are expressed at higher molar concentrations. We refer to these as low-abundance miRNAs (miR-134, miR-212, and miR-132) and high-abundance miRNAs (miR-138, miR-128, and miR-124), respectively (Fig 4A).

When determining the relative effects of the lentiviral targets on TDMD and miRNA-mediated mRNA decay for all six miRNAs, we found that TDMD appeared to be generally more efficient for low- than for high-abundance miRNAs (Fig 4B, 4× targets, lower left quadrant). One exception was miR-134, which, for unknown reasons, was less susceptible to TDMD than anticipated based on its low abundance. To examine the influence of miRNA abundance on TDMD under more defined conditions, we tested the consequences of increasing miR-132 concentration beyond its normally moderate endogenous level. To this end, we transduced a pri-miR-132 construct at increasing MOIs to achieve amounts comparable to the more abundant miRNAs (Fig 4C). Consistent with the findings for endogenous miRNAs of varying abundance, increasing miR-132 levels caused decreasing TDMD effects (Fig 4D, lower left quadrant).

We further examined the extent of target mRNA degradation induced by endogenous miRNAs of varying abundance and miR-132 supplied at different levels. We observed consistently that low-abundance miRNAs induced virtually no mRNA decay, whereas high-abundance miRNAs triggered efficient decay of the target mRNAs (Fig 4B and D, upper left quadrants). The extent of TDMD is thus inverse to the extent of miRNA-mediated mRNA decay. These results argue against a model where the miRNA and its target are co-degraded in TDMD. Instead, TDMD and target degradation appear to be two independent processes whose balance can be shifted by alterations in miRNA abundance.

 

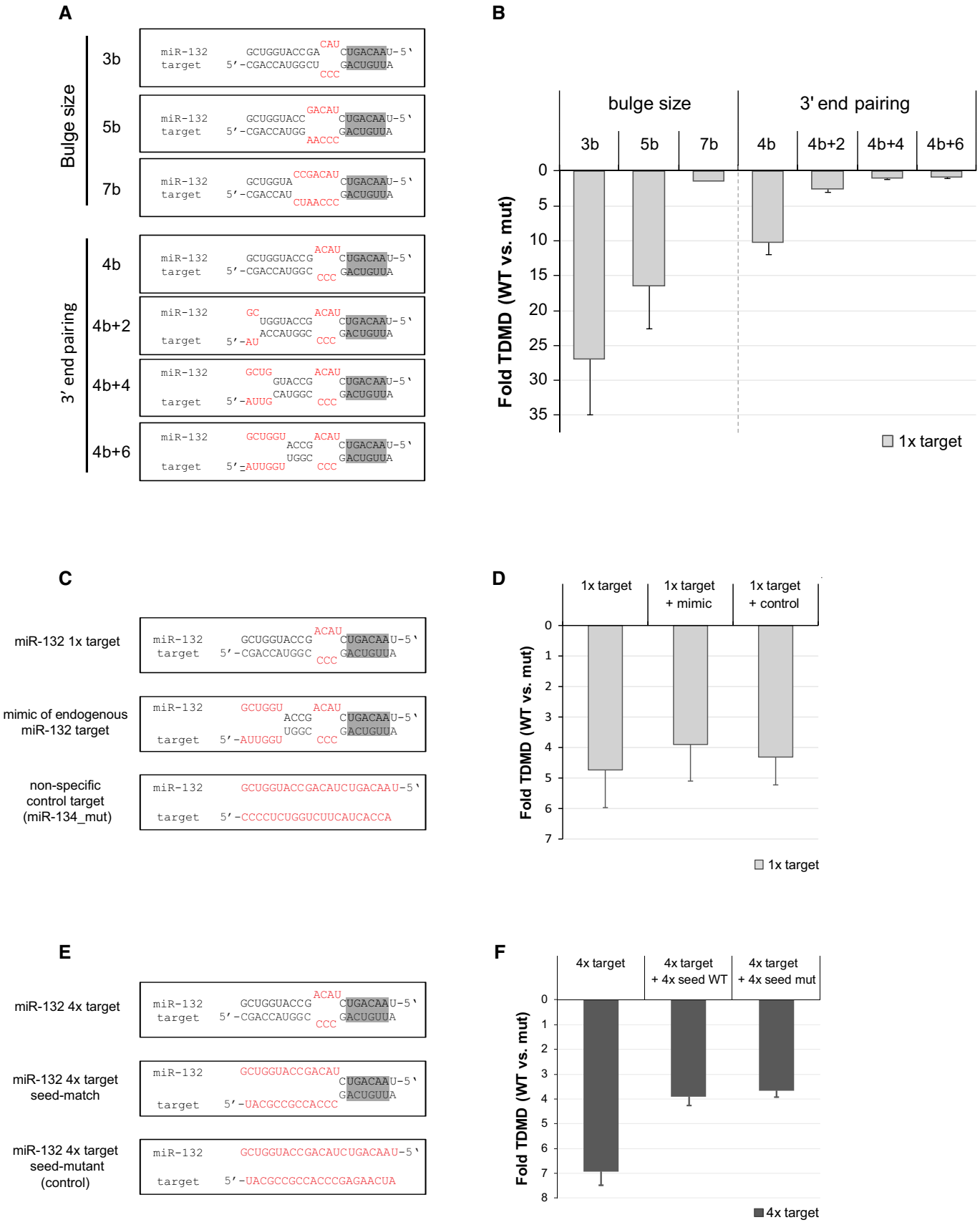
A
Bulge size
3b
5b
7b
3' end pairing
4b
4b+2
4b+4
4b+6
miR-132
target
B
bulge size
3' end pairing
3b
5b
7b
4b
4b+2
4b+4
4b+6
Fold TDMD (WT vs. mut)
1x target
C
miR-132 1x target
mimic of endogenous miR-132 target
non-specific control target (miR-134_mut)
D
1x target
1x target + mimic
1x target + control
Fold TDMD (WT vs. mut)
1x target
E
miR-132 4x target
miR-132 4x target seed-match
miR-132 4x target seed-mutant (control)
F
4x target
4x target + 4x seed WT
4x target + 4x seed mut
Fold TDMD (WT vs. mut)
4x target

**Figure 3.**

**Figure 3. Canonical miRNA target sites can neither induce nor compete with TDMD.**

A, B TDMD ($n$ = 2, each with two technical replicates from independent infections) for miR-132 in the presence of the depicted 1× targets. Fold TDMD effects were calculated relative to a miR-132 mut target.

C, D TDMD ($n$ = 2, each with two technical replicates from independent infections) for miR-132 in the presence of a 1× target with extensively complementary binding sites alone or in combination with a natural 1× target analogue that contains seed pairing plus 3′-supplementary region. A non-specific target with mut binding sites for miR-134 was used as a negative control. Fold TDMD effects were calculated relative to a miR-132 mut target.

E, F TDMD ($n$ = 1, with two technical replicates from independent infections) for miR-132 in the presence of a 4× target with extensively complementary binding sites alone or in combination with 4× targets containing seed-pairing binding sites. A mut target was used as a negative control.

Data information: Schematics of miR-132 binding sites present in (A) artificial 1× targets, (C) the 3′-UTRs of genes reported as natural targets of miR-132, and (E) additional predicted target sites [24], respectively. Seed-pairing regions are highlighted in gray. Fold TDMD effects were calculated relative to a miR-132 mut target. Shown are means ± s.e.m.

### Multiple target sites support cooperative degradation of the target mRNA but not the miRNA

The experiments presented above involved targets with four binding sites, and it was previously shown that multiple miRNA binding sites induce a cooperative effect on miRNA-mediated repression [25–28]. Whether such effects play a role in determining TDMD efficacy is not known. We therefore asked which process, TDMD or mRNA repression, would predominate if we prevented cooperativity by using targets with only a single miRNA binding site (1× targets). In clear contrast to the 4× target results, 1× targets induced a significant (threefold to sevenfold) TDMD for all six miRNAs tested, irrespective of the miRNA abundance (Fig 4B, lower right quadrant). Conversely, virtually no mRNA decay for the respective 1× targets was induced by any of the tested miRNAs (Fig 4B, upper right quadrant). Similarly, a 1× target of miR-132 induced a robust TDMD response across a range of miR-132 levels, whereas neither mRNA decay (Fig 4D, upper right quadrant) nor translational repression (Supplementary Fig S4C and D) of the target occurred at even the highest miR-132 level. We conclude that TDMD and miRNA-mediated target silencing and degradation are independent processes and that only the latter is strongly dependent on cooperativity. Hence, eliminating cooperativity by reducing target site number shifts the balance toward TDMD, permitting extensive clearance of even abundant miRNAs.

### TDMD appears to be a multiple turnover process in neurons

To quantify better the efficiencies of TDMD and mRNA decay, we estimated the absolute average numbers of miR-132 and target molecules degraded per cell in the different conditions (Fig 4E and F; Materials and Methods). We determined these numbers, ΔmiR and Δtarget, by calculating the difference in the amount of respective molecules in cells expressing a mut versus a wild-type target. As we increased the pri-miR-132 concentration, ΔmiR also increased. This was true for both the 1× and the 4× targets at increasing pri-miR-132 concentrations (Fig 4E), despite the fact that the fold TDMD changes decrease with increasing miR-132 levels for the 4× target (Fig 4D, lower left quadrant). This apparent inconsistency is explained by the fact that the fold TDMD is a relative measure of efficacy (i.e. a ratio). Strikingly, at high miRNA levels, the number of miRNA molecules degraded exceeded the initial number of target mRNA molecules expressed in the neurons (Fig 4E), such that for instance ~3,300 1× target mRNA molecules sufficed to induce degradation of ~16,000 miR-132 molecules. Similarly, a starting amount of 3,300 4× targets sufficed for degradation of ~12,000 miR-132 molecules, which is even more remarkable when considering that miR-132 eliminates > 90% of the targets under these conditions (Fig 4D, lower left quadrant). (Note that miR-132 initial levels in this experiment greatly surpass the endogenous levels of an abundant miRNA such as miR-124.) Hence, the true potency of the miRNA degradation machinery in neurons is likely even higher than estimated in these experiments. Collectively, these results suggest that an individual mRNA molecule can induce decay of more than one miRNA molecule. Because miR-132 and its artificial mutant target appear to be made, and also destroyed, at approximately similar rates (Supplementary Fig S5), we conclude that TDMD in neurons exhibits the hallmarks of a multiple turnover process.

### TDMD is particularly active in primary neurons

The strong activity of TDMD in neurons prompted us to examine its efficacy in other cell types. To that end, we transduced or transfected

**Figure 4. TDMD is likely multiple turnover and does not rely on target site cooperativity.**

A Absolute levels of endogenous miRNA determined by RT–qPCR in the presence of mut targets (Fig 1A) provided by transduction of lentiviruses at an MOI of ~1.

B TDMD and miRNA-mediated decay calculated in the presence (MOI of ~1) of 1× or 4× targets, respectively, against the indicated endogenous miRNAs. miRNA binding sites follow the same architecture as is shown in Fig 1A.

C Absolute miR-132 levels determined by RT–qPCR after transducing neurons with a mut target (MOI of ~1) against miR-132 in the absence (only endogenous miR-132 levels) or presence of increasing amounts of a pri-miR-132-expressing lentiviral transgene (MOI of ~1, 3, and 10, respectively).

D Fold TDMD and fold miRNA-mediated decay effects calculated in the presence of 1× or 4× targets against miR-132 (MOI of ~1), at increasing MOIs of a pri-miR-132-expressing lentiviral transgene (as indicated in C). *$P < 0.05$; **$P < 0.01$ ($P$-values for mRNA decay: $P = 0.01$ for endogenous versus MOI 3; $P = 0.003$ for endogenous versus MOI 10. $P$-values for TDMD: $P = 0.03$ for endogenous versus MOI 1; $P = 0.01$ for endogenous versus MOI 3; $P = 0.004$ for endogenous versus MOI 10). $P$-values were calculated by using an independent two-sample $t$-test.

E, F Total number of degraded (E) miR-132 molecules/cell and (F) target mRNA molecules/cell calculated from experiments in (D).

Data information: A dashed line in (A, C, E) indicates the median mRNA expression value of the mut target determined by RT–qPCR. Fold TDMD and mRNA decay changes were calculated relative to mut targets. Shown are means ± s.e.m.; $n = 3$.
Source data are available online for this figure.

 

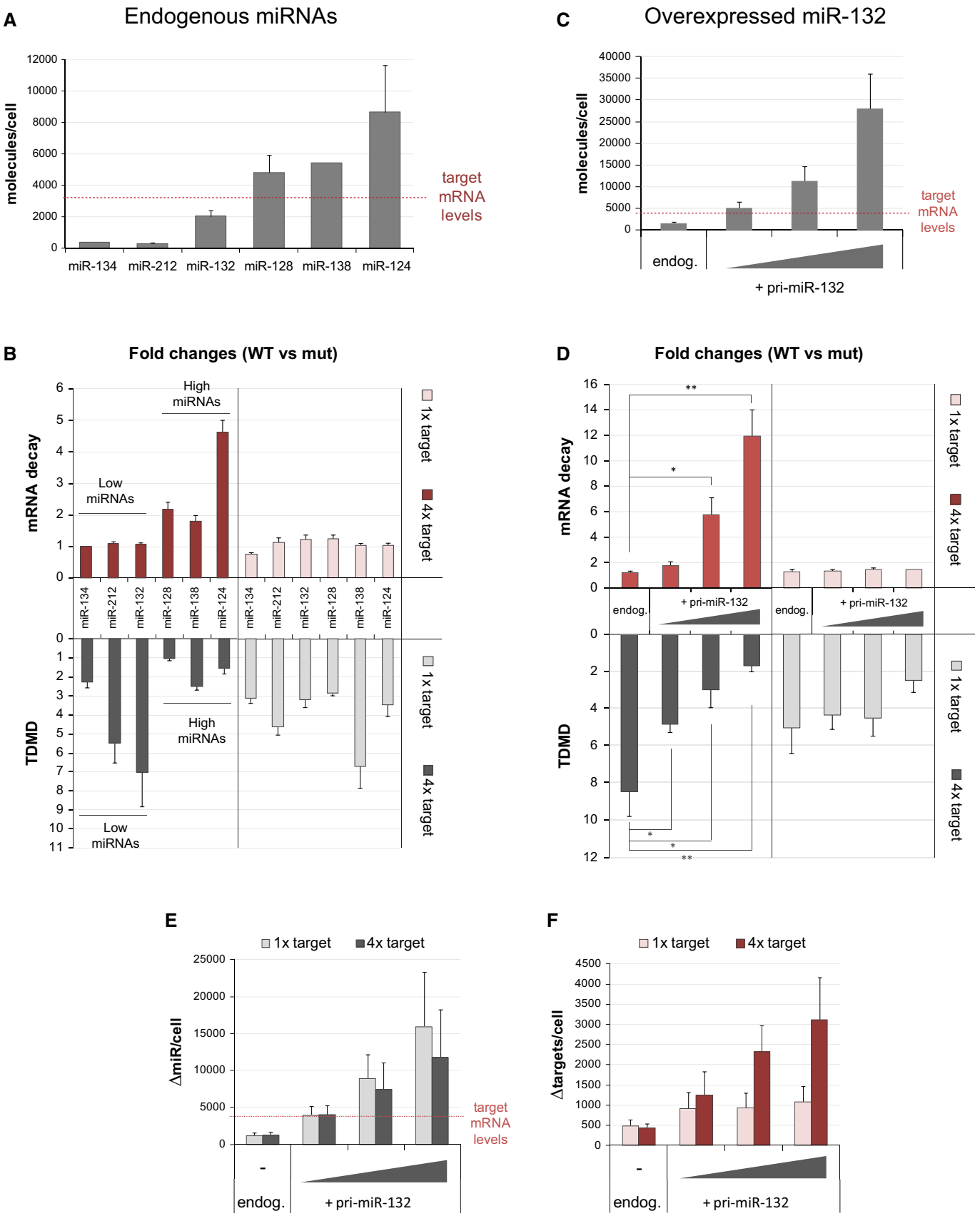


**Figure 4.**

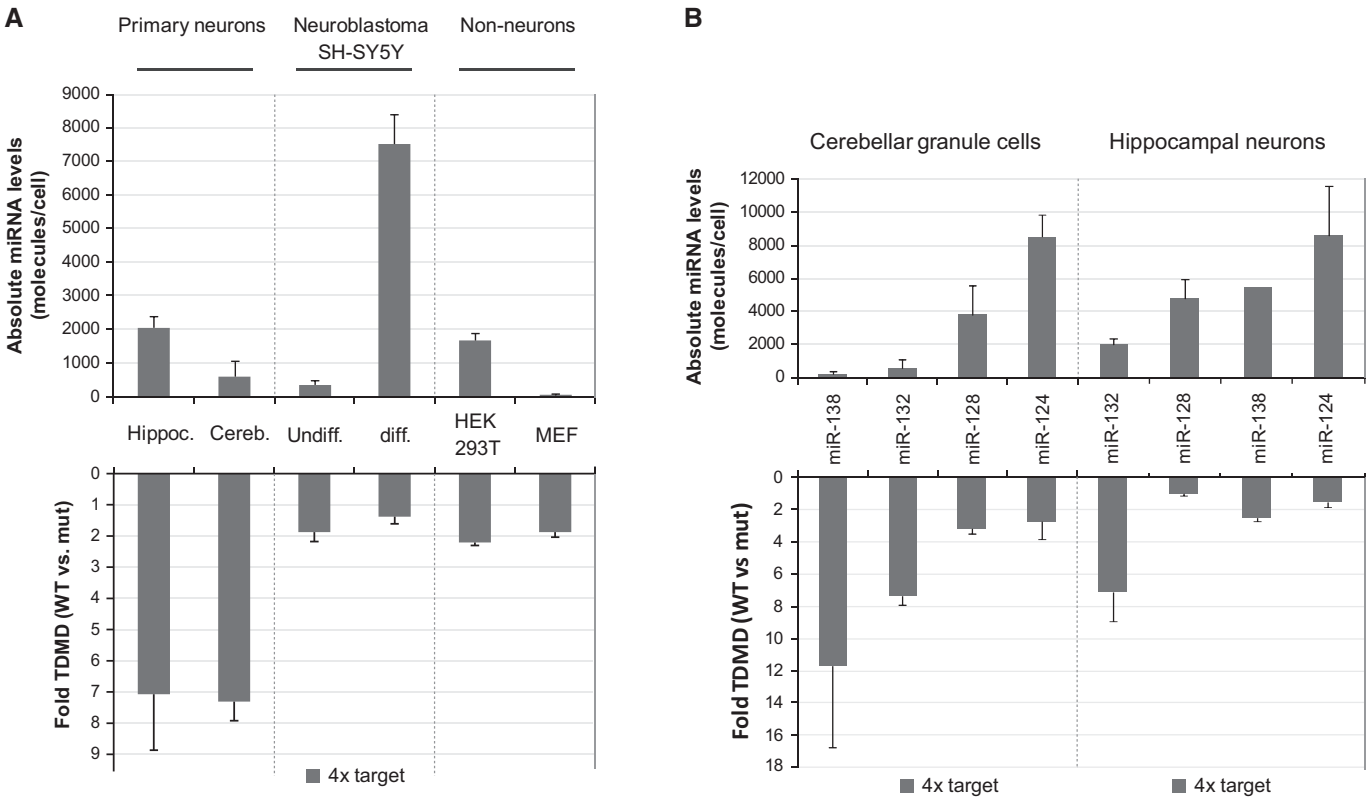


**Figure 5. TDMD is particularly active in primary neurons.**

A, B TDMD and absolute miRNA levels (mean ± s.e.m.) calculated in the presence of 4× targets against (A) miR-132 and (B) additional miRNAs for different cell types. (A) Hippoc., rat primary hippocampal neurons ($n$ = 3); Cereb., primary mouse cerebellar granule cells ($n$ = 2, each with two technical replicates from independent infections); non-differentiated ($n$ = 3) or differentiated ($n$ = 2, each with two technical replicates from independent infections) SH-SY5Y neuroblastoma cells; MEF ($n$ = 2, each with two technical replicates from independent infections), primary mouse embryonic fibroblasts. HEK-293T cells ($n$ = 3) were co-transfected with a plasmid expressing pri-miR-132. (B) Primary mouse cerebellar granule cells ($n$ = 2, each with two technical replicates from independent infections) and hippocampal neurons ($n$ = 3). Fold changes were calculated relative to a mut target.

Source data are available online for this figure.

a transgene with 4× sites against miR-132 into primary rat hippocampal neurons, primary mouse cerebellar granule neurons, undifferentiated or differentiated human SH-SY5Y neuroblastoma cells, HEK-293T cells, and primary mouse embryonic fibroblasts (MEF). In the case of HEK-293T cells, which lack endogenous miR-132, pri-miR-132 was expressed from a co-transfected plasmid. In each case, the target was present in excess of the miRNA in order to allow for a direct comparison between cell types. TDMD was significantly more efficient in the primary rat hippocampal neurons and the primary mouse cerebellar granule neurons than in the other cell types (Fig 5A). This was not due to lower miR-132 abundance in the primary neurons (Fig 5A). Indeed, TDMD remained poorly active in HEK-293T cells even in the presence of more than tenfold excess of target and irrespective of the use of 1× or 4× targets (Supplementary Fig S6). Further comparison of TDMD in primary rat hippocampal neurons and primary mouse cerebellar granule neurons revealed very similar responses for all four different miRNAs tested (Fig 5B). Even though the abundance of the different miRNAs does not follow the same order in both types of neurons, the relative efficiency of TDMD was anticorrelated with miRNA levels (Fig 5B).

From these results, we conclude that miRNA degradation induced by highly complementary targets is highly effective in primary neurons but much less so in non-neuronal cells or established neuronal cell lines. This is most striking considering that primary neurons are post-mitotic cells, implying that the measured effect is not an indirect result of the dilution of miRNAs due to cell division.

## Discussion

The size and dynamic activity of neurons necessitate rapid and local regulation of gene expression [29]. Hence, miRNA function in the brain is of particular interest [30]. However, because long half-lives limit the suitability of miRNAs for dynamic gene expression changes [2], mechanisms are needed for their destabilization. Here, we have shown that neurons can initiate a potent and specific miRNA degradation response upon expression of highly complementary target mRNAs. The efficacy of this TDMD process appears to be a consequence of multiple turnover activity. The ability of individual target mRNA molecules to induce decay of multiple miRNA molecules also

 

rules out mechanisms that involve co-degradation of the miRNA and its target, and this conclusion is corroborated by our observation that TDMD induced by single-site targets occurs without appreciable target RNA decay.

Although TDMD and miRNA-mediated target silencing both require base-pairing between a miRNA and its target, we find target site cooperativity only for mRNA silencing but not for TDMD. Thus, targets with either one (1×) and four (4×) miRNA binding sites induce TDMD, but mRNA silencing occurs only in response to 4× targets. An important implication is that, somewhat counterintutively, depletion of abundant miRNAs is more, rather than less, effective when only a single instead of multiple miRNA sites is present in target RNA. This knowledge may thus guide the harnessing of TDMD to knock down miRNAs in experimental settings.

A second, unrelated implication concerns the nature of cooperativity of mRNA silencing, which, in principle, might operate at the level of either miRNA binding or miRNA function [28]. The distinction between TDMD and mRNA silencing when quantified here in the same experiment, with the same targets, is inconsistent with binding cooperativity, suggesting instead functional cooperativity. Although the mechanisms remain to be elucidated, it is conceivable that the presence of multiple miRISC complexes on a single target facilitates interaction with GW182 or other silencing proteins acting downstream of Argonautes.

The potency of TDMD in directing miRNA elimination combined with the precedence of viruses using TDMD to degrade host cell miRNAs further suggests strongly that TDMD is also a physiologically relevant process in neurons. The mechanistic insights gained through the present study and listed below may help to guide future identification of relevant situations and TDMD-inducing RNAs. First, similar to other instances of TDMD [3,10,12,13,15,16], inducers require incomplete but extensive target complementarity. Thus, a central bulge of $\leq 5$ nt and a maximum of two mismatches to the 3′-end of the miRNA are the minimal base-pairing requirements for efficacious TDMD. Speculatively, the high efficacy of TDMD observed in neurons might have shaped evolution of miRNA binding sites by restricting their complementarity [31], explaining why TDMD-type miRNA binding sites occur with such low frequency in animals [32]. In line with this idea, canonical targets with limited complementarity are not only incapable of eliciting TDMD themselves but also fail to compete efficiently with highly complementary targets to attenuate TDMD. Second, TDMD-inducing RNAs need to resolve a conundrum, namely that miRNA-mediated regulation is most relevant for the abundant, active miRNAs in a cell [33,34], but that these are also the ones that will destroy TDMD inducers. Structures resistant to degradation, such as the recently reported endogenous circular RNAs [35–37], or the highly structured designer Tough Decoys RNAs [38,39] may offer a potential solution. Alternatively, and as demonstrated here, a target with a single rather than multiple binding sites can escape silencing by the miRNA without compromising TDMD activity. Third, although abundant TDMD inducers may be at an advantage when degradation of highly abundant miRNAs such as miR-124 is sought, the multiple turnover activity provides significant miRNA decay even when inducers are present at substoichiometric levels.

Although target-directed tailing of miRNAs has been observed in several systems [3,12,15], its role in TDMD has remained unknown. Thus, although adenylation and uridylation have been linked to miRNA stability in both plants and animals [40–44], perfectly complementary targets of siRNAs sufficed for ejection of these miRNA-like molecules from Ago without a need for tailing *in vitro* [19]. Similarly, MCMV-infected NIH-3T3 cells exhibit enhanced tailing of miR-27 in total RNA, but not on Ago2-loaded miRNAs [12], consistent with tailing occuring subsequent to miRNA eviction from Ago, or happening on Ago2-bound miRNAs but leading to their immediate release from RISC. By contrast, we find tailing during TDMD to occur on Ago-bound miRNAs and to coincide with degradation. Moreover, it appears that the mature (untailed) miRNA isoform is more extensively depleted from the Ago-associated than the total RNA pool (Fig 2B and Supplementary Fig S2D). Hence, it seems possible that tailing of Ago-bound miRNAs is a first step in a pathway that ultimately leads to ejection and degradation of the miRNA. Whether the discrepancy to the earlier work that reported the preferential induction of tailed miRNAs outside Ago [12] reflects true biological differences remains to be determined. At any rate, tailed species of small RNAs have been detected on Argonaute proteins from plants and animals [45–47], demonstrating that, consistent with our observations, tailing does not require dissociation of the miRNA from Ago.

Finally, the differences that our comparative study revealed for TDMD activity among different mammalian cells were unexpected and striking: Whereas TDMD is highly effective in two types of primary neurons, rat hippocampal neurons and mouse cerebellar granule cells, little activity was observed in either a neuroblastoma (even following differentiation) or an embryonic kidney cell line. Although the latter two are neither primary cells nor of rodent origin, these distinctions fail to explain the difference in TDMD activity since primary mouse embryonic fibroblasts (MEF) displayed equally muted TDMD activity. Hence, it appears to be some feature of being a primary neuronal cell that promotes effective TDMD. Although the molecular basis of this observation remains to be determined, it might reflect the general increase in miRNA metabolism in these cells [7–9]. Conversely, elevated TDMD activity in neurons appears well matched to the extensive reliance of the nervous system on highly dynamic and spatially localized regulation [29]. Thus, TDMD emerges as a suitable mechanism for selective recognition, release, and degradation of specific miRNAs in neurons.

## Materials and Methods

Procedures are detailed in the Supplementary Information.

#### Plasmid construction

Lentiviral vectors bearing the human Syn promoter are based on pRRLSIN.cPPT.PGK-GFP.WPRE (Addgene plasmid 12252). Lentiviral vectors with the tetracycline-inducible promoter (TREp) are based on the plasmid SYN-Tetoff-GFP [48]. Plasmids expressing pri-miR-132 and pri-miR-182 are based on miRNASelect™ pEGP-mmu-mirna expression vectors (Cell Biolabs). The lentiviral vector driving expression of FLAG/HA-Ago2 (human) from the Syn promoter (pLV-FLAG-HA_Ago2) was generated by amplifying FLAG/HA-Ago2 from pIRESneo-FLAG/HA Ago2 (Addgene plasmid 10822).

#### Design of artificial miRNA binding sites of target constructs

The miRNA binding region consists on extensively complementary sites with bulged nucleotides at positions 9–12 to prevent cleavage of the RNA. Sequences of spacers and bulges were optimized to have random nucleotide composition and to keep the miRNA binding region unstructured.

#### Lentivirus production

Lentiviral particles were produced in HEK-293T cells with the packaging vectors pMD2.G (Addgene plasmid 12259) and pCMVR8.74 (Addgene plasmid 22036).

#### Neuronal cultures

Primary rat hippocampal neurons and mouse cerebellar granule cells were prepared as previously described [49,50].

#### RT–qPCR quantification

Mature miRNA, miRNA*, and U6 levels were determined by using TaqMan microRNA Assays (Applied Biosystems).

#### Small RNA sequencing and data analysis

Small RNA libraries were prepared using Illumina TruSeq Small RNA kits (Cat # RS-200-0024). miRNA expression levels were calculated and normalized as described previously [51] using rat miRBase (http://www.mirbase.org/) release 20 as a reference [18].

#### Accession numbers

All sequencing data generated for this study have been deposited in NCBI's Gene Expression Omnibus [52] and are accessible through GEO Series accession number GSE57663.

**Supplementary information** for this article is available online: http://embor.embopress.org


### Acknowledgements

We thank Heike Brinkhaus and Jacek Krol for helping with rat hippocampal neuron cultures, Patrick Kopp for preparing the MEF cultures, Stephan Duss and Nicola Aceto for helping with lentivirus preparation, Kirsten Jacobeit and Sophie Dessus-Babus for library preparation and sequencing, Francisco G. Scholl and Michael A. Kiebler for providing materials, and Takashi Miki and Florian Aeschimann for a critical reading of the manuscript. HG has received funding for the research leading to these results from the European Union Seventh Framework Programme (FP7/2007-2013) under grant agreement no 241985 (European Research Council "miRTurn"), the NCCR RNA & Disease funded by the Swiss National Science Foundation, and the Novartis Research Foundation through the FMI. MdlM was a recipient of postdoctoral fellowships from Human Frontier Science Program (LT000087/2009-L) and Peter und Traudl Engelhorn-Stiftung.


### Author contributions

MdlM conceived the project and designed, performed, and interpreted the experiments. DG performed all bioinformatics analysis and interpreted the data. MV conducted most of the tissue culture work and performed several experiments. MBS designed the artificial miRNA binding sites of target constructs. CW prepared the cerebellar granule cultures and discussed experimental strategies. PS discussed the design of some experiments. WF and HG discussed the design and interpretation of experiments and co-supervised the whole project. The manuscript was written by MdlM, WF, and HG.

### Conflict of interest

The authors declare that they have no conflict of interest.

## References


1. Krol J, Loedige I, Filipowicz W (2010) The widespread regulation of microRNA biogenesis, function and decay. *Nat Rev Genet* 11: 597 – 610
2. Hausser J, Syed AP, Selevsek N, van Nimwegen E, Jaskiewicz L, Aebersold R, Zavolan M (2013) Timescales and bottlenecks in miRNA-dependent gene regulation. *Mol Syst Biol* 9: 711
3. Baccarini A, Chauhan H, Gardner TJ, Jayaprakash AD, Sachidanandam R, Brown BD (2011) Kinetic analysis reveals the fate of a microRNA following target regulation in mammalian cells. *Curr Biol* 21: 369 – 376
4. Gatfield D, Le Martelot G, Vejnar CE, Gerlach D, Schaad O, Fleury-Olela F, Ruskeepaa AL, Oresic M, Esau CC, Zdobnov EM *et al* (2009) Integration of microRNA miR-122 in hepatic circadian gene expression. *Genes Dev* 23: 1313 – 1326
5. Hwang HW, Wentzel EA, Mendell JT (2007) A hexanucleotide element directs microRNA nuclear import. *Science* 315: 97 – 100
6. van Rooij E, Sutherland LB, Qi X, Richardson JA, Hill J, Olson EN (2007) Control of stress-dependent cardiac growth and gene expression by a microRNA. *Science* 316: 575 – 579
7. Krol J, Busskamp V, Markiewicz I, Stadler MB, Ribi S, Richter J, Duebel J, Bicker S, Fehling HJ, Schubeler D *et al* (2010) Characterizing light-regulated retinal microRNAs reveals rapid turnover as a common property of neuronal microRNAs. *Cell* 141: 618 – 631
8. Rajasethupathy P, Fiumara F, Sheridan R, Betel D, Puthanveettil SV, Russo JJ, Sander C, Tuschl T, Kandel E (2009) Characterization of small RNAs in Aplysia reveals a role for miR-124 in constraining synaptic plasticity through CREB. *Neuron* 63: 803 – 817
9. Sethi P, Lukiw WJ (2009) Micro-RNA abundance and stability in human brain: specific alterations in Alzheimer's disease temporal lobe neocortex. *Neurosci Lett* 459: 100 – 104
10. Cazalla D, Yario T, Steitz JA (2010) Down-regulation of a host microRNA by a *Herpesvirus saimiri* noncoding RNA. *Science* 328: 1563 – 1566
11. Buck AH, Perot J, Chisholm MA, Kumar DS, Tuddenham L, Cognat V, Marcinowski L, Dolken L, Pfeffer S (2010) Post-transcriptional regulation of miR-27 in murine cytomegalovirus infection. *RNA* 16: 307 – 315
12. Marcinowski L, Tanguy M, Krmpotic A, Rädle B, Lisnic VJ, Tuddenham L, Chane-Woon-Ming B, Ruzsics Z, Erhard F, Benkartek C *et al* (2012) Degradation of cellular miR-27 by a novel, highly abundant viral transcript is important for efficient virus replication *in vivo*. *PLoS Pathog* 8: e1002510
13. Lee S, Song J, Kim S, Kim J, Hong Y, Kim Y, Kim D, Baek D, Ahn K (2013) Selective degradation of host microRNAs by an intergenic HCMV noncoding RNA accelerates virus production. *Cell Host Microbe* 13: 678 – 690
14. Rissland Olivia S, Hong S-J, Bartel David P (2011) MicroRNA destabilization enables dynamic regulation of the miR-16 family in response to cell-cycle changes. *Mol Cell* 43: 993 – 1004


 

15. Ameres SL, Horwich MD, Hung JH, Xu J, Ghildiyal M, Weng Z, Zamore PD (2010) Target RNA-directed trimming and tailing of small silencing RNAs. *Science* 328: 1534 – 1539
16. Libri V, Helwak A, Miesen P, Santhakumar D, Borger JG, Kudla G, Grey F, Tollervey D, Buck AH (2012) Murine cytomegalovirus encodes a miR-27 inhibitor disguised as a target. *Proc Natl Acad Sci USA* 109: 279 – 284
17. McNeill E, Van Vactor D (2012) MicroRNAs shape the neuronal landscape. *Neuron* 75: 363 – 379
18. Kozomara A, Griffiths-Jones S (2014) miRBase: annotating high confidence microRNAs using deep sequencing data. *Nucleic Acids Res* 42: D68 – D73
19. De N, Young L, Lau P-W, Meisner N-C, Morrissey DavidÂ V, MacRae IanÂ J (2013) Highly complementary target RNAs promote release of guide RNAs from human argonaute2. *Mol Cell* 50: 344 – 355
20. Bartel DP (2009) MicroRNAs: target recognition and regulatory functions. *Cell* 136: 215 – 233
21. Vo N, Klein ME, Varlamova O, Keller DM, Yamamoto T, Goodman RH, Impey S (2005) A cAMP-response element binding protein-induced microRNA regulates neuronal morphogenesis. *Proc Natl Acad Sci USA* 102: 16426 – 16431
22. Anand S, Majeti BK, Acevedo LM, Murphy EA, Mukthavaram R, Scheppke L, Huang M, Shields DJ, Lindquist JN, Lapinski PE *et al* (2010) MicroRNA-132-mediated loss of p120RasGAP activates the endothelium to facilitate pathological angiogenesis. *Nat Med* 16: 909 – 914
23. Ucar A, Vafaizadeh V, Jarry H, Fiedler J, Klemmt PAB, Thum T, Groner B, Chowdhury K (2010) miR-212 and miR-132 are required for epithelial stromal interactions necessary for mouse mammary gland development. *Nat Genet* 42: 1101 – 1108
24. Lewis BP, Shih IH, Jones-Rhoades MW, Bartel DP, Burge CB (2003) Prediction of mammalian microRNA targets. *Cell* 115: 787 – 798
25. Grimson A, Farh KK-H, Johnston WK, Garrett-Engele P, Lim LP, Bartel DP (2007) MicroRNA targeting specificity in mammals: determinants beyond seed pairing. *Mol Cell* 27: 91 – 105
26. Saetrom P, Heale BSE, Snove O, Aagaard L, Alluin J, Rossi JJ (2007) Distance constraints between microRNA target sites dictate efficacy and cooperativity. *Nucleic Acids Res* 35: 2333 – 2342
27. Wu E, Thivierge C, Flamand M, Mathonnet G, Vashisht AA, Wohlschlegel J, Fabian MR, Sonenberg N, Duchaine TF (2010) Pervasive and cooperative deadenylation of 3′ UTRs by embryonic microRNA families. *Mol Cell* 40: 558 – 570
28. Broderick JA, Salomon WE, Ryder SP, Aronin N, Zamore PD (2011) Argonaute protein identity and pairing geometry determine cooperativity in mammalian RNA silencing. *RNA* 17: 1858 – 1869
29. Holt CE, Schuman EM (2013) The central dogma decentralized: new perspectives on RNA function and local translation in neurons. *Neuron* 80: 648 – 657
30. Schratt G (2009) microRNAs at the synapse. *Nat Rev Neurosci* 10: 842 – 849
31. Ameres SL, Zamore PD (2013) Diversifying microRNA sequence and function. *Nat Rev Mol Cell Biol* 14: 475 – 488
32. Farh KK, Grimson A, Jan C, Lewis BP, Johnston WK, Lim LP, Burge CB, Bartel DP (2005) The widespread impact of mammalian MicroRNAs on mRNA repression and evolution. *Science* 310: 1817 – 1821
33. Brown BD, Gentner B, Cantore A, Colleoni S, Amendola M, Zingale A, Baccarini A, Lazzari G, Galli C, Naldini L (2007) Endogenous microRNA can be broadly exploited to regulate transgene expression according to tissue, lineage and differentiation state. *Nat Biotechnol* 25: 1457 – 1467
34. Mullokandov G, Baccarini A, Ruzo A, Jayaprakash AD, Tung N, Israelow B, Evans MJ, Sachidanandam R, Brown BD (2012) High-throughput assessment of microRNA activity and function using microRNA sensor and decoy libraries. *Nat Methods* 9: 840 – 846
35. Salzman J, Gawad C, Wang PL, Lacayo N, Brown PO (2012) Circular RNAs are the predominant transcript isoform from hundreds of human genes in diverse cell types. *PLoS ONE* 7: e30733
36. Hansen TB, Jensen TI, Clausen BH, Bramsen JB, Finsen B, Damgaard CK, Kjems J (2013) Natural RNA circles function as efficient microRNA sponges. *Nature* 495: 384 – 388
37. Memczak S, Jens M, Elefsinioti A, Torti F, Krueger J, Rybak A, Maier L, Mackowiak SD, Gregersen LH, Munschauer M *et al* (2013) Circular RNAs are a large class of animal RNAs with regulatory potency. *Nature* 495: 333 – 338
38. Xie J, Ameres SL, Friedline R, Hung JH, Zhang Y, Xie Q, Zhong L, Su Q, He R, Li M *et al* (2012) Long-term, efficient inhibition of microRNA function in mice using rAAV vectors. *Nat Methods* 9: 403 – 409
39. Haraguchi T, Ozaki Y, Iba H (2009) Vectors expressing efficient RNA decoys achieve the long-term suppression of specific microRNA activity in mammalian cells. *Nucleic Acids Res* 37: e43
40. Ramachandran V, Chen X (2008) Degradation of microRNAs by a family of exoribonucleases in Arabidopsis. *Science* 321: 1490 – 1492
41. Li J, Yang Z, Yu B, Liu J, Chen X (2005) Methylation protects miRNAs and siRNAs from a 3′-end uridylation activity in Arabidopsis. *Curr Biol* 15: 1501 – 1507
42. Shen B, Goodman HM (2004) Uridine addition after microRNA-directed cleavage. *Science* 306: 997
43. Jones MR, Quinton LJ, Blahna MT, Neilson JR, Fu S, Ivanov AR, Wolf DA, Mizgerd JP (2009) Zcchc11-dependent uridylation of microRNA directs cytokine expression. *Nat Cell Biol* 11: 1157 – 1163
44. Katoh T, Sakaguchi Y, Miyauchi K, Suzuki T, Kashiwabara S, Baba T (2009) Selective stabilization of mammalian microRNAs by 3′ adenylation mediated by the cytoplasmic poly(A) polymerase GLD-2. *Genes Dev* 23: 433 – 438
45. Zhai J, Zhao Y, Simon SA, Huang S, Petsch K, Arikit S, Pillay M, Ji L, Xie M, Cao X *et al* (2009) Plant microRNAs display differential 3′ truncation and tailing modifications that are ARGONAUTE1 dependent and conserved across species. *Plant Cell* 25: 2417 – 2428
46. van Wolfswinkel JC, Claycomb JM, Batista PJ, Mello CC, Berezikov E, Ketting RF (2009) CDE-1 affects chromosome segregation through uridylation of CSR-1-bound siRNAs. *Cell* 139: 135 – 148
47. Dueck A, Ziegler C, Eichner A, Berezikov E, Meister G (2012) microRNAs associated with the different human Argonaute proteins. *Nucleic Acids Res* 40: 9850 – 9862
48. Gascón S, Paez-Gomez JA, Diaz-Guerra M, Scheiffele P, Scholl FG (2008) Dual-promoter lentiviral vectors for constitutive and regulated gene expression in neurons. *J Neurosci Methods* 168: 104 – 112
49. Chih B, Engelman H, Scheiffele P (2005) Control of excitatory and inhibitory synapse formation by neuroligins. *Science* 307: 1324 – 1328
50. Hatten ME (1985) Neuronal regulation of astroglial morphology and proliferation *in vitro*. *J Cell Biol* 100: 384 – 396
51. Miki TS, Ruegger S, Gaidatzis D, Stadler MB, Grosshans H (2014) Engineering of a conditional allele reveals multiple roles of XRN2 in *Caenorhabditis elegans* development and substrate specificity in microRNA turnover. *Nucleic Acids Res* 42: 4056 – 4067
52. Edgar R, Domrachev M, Lash AE (2002) Gene expression omnibus: NCBI gene expression and hybridization array data repository. *Nucleic Acids Res* 30: 207 – 210